(35)

ELSEVIER

Signal Processing 80 (2000) 1217–1229

SIGNAL PROCESSING

www.elsevier.nl/locate/sigpro

Sensitivity of orthogonal frequency-division multiplexed systems to carrier and clock synchronization errors

Heidi Steendam, Marc Moeneclaey*

Telecommunications and Information Processing Dept., Ghent University, Sint-Pietersnieuwstraat 41, B-9000 Gent, Belgium

Received 28 November 1997

Abstract

In this contribution, we present an overview of research results pertaining to the sensitivity of orthogonal frequency-division multiplexed (OFDM) systems to synchronization errors. We show that OFDM systems are quite sensitive to *carrier frequency offset* and *clock frequency offset*: in the presence of these impairments, the signal-to-noise ratio (SNR) at the input of the decision device is a decreasing function of the number of carriers. On the other hand, *carrier phase jitter* and *timing jitter* give rise to a degradation of the SNR at the input of the decision device which does not depend on the number of carriers; as compared to traditional single-carrier systems, OFDM systems have the same sensitivity to carrier phase jitter and a somewhat larger sensitivity to timing jitter. © 2000 Elsevier Science B.V. All rights reserved.

Zusammenfassung

In diesem Beitrag stellen wir eine Übersicht von Forschungsergebnissen vor, die sich auf die Empfindlichkeit orthogonaler Frequenzmultiplexsysteme (OFDM) gegenüber Synchronisationsfehlern beziehen. Wir zeigen, daß OFDM-Systeme gegenüber Trägerfrequenzversatz und Abtastfrequenzversatz ziemlich empfindlich sind: bei Vorliegen dieser Störungen ist das Signal-zu-Rauschleistungsverhaltnis (SNR) am Eingang des Entscheiders eine abnehmende Funktion von der Anzahl der Trägerfrequenzen. Andererseits verursachen zufällige Abweichungen von der Trägerphase und der Abtastphase eine Verschlechterung des SNR am Entscheidereingang, die nicht von der Anzahl der Trägerfrequenzen abhängt. Verglichen mit gewöhnlichen Einzelträgersystemen haben OFDM-Systeme die gleiche Empfindlichkeit gegenüber zufälligen Abweichungen der Trägerphase und eine etwas größere Empfindlichkeit gegenüber zufälligen Abweichungen der Abtastphase. © 2000 Elsevier Science B.V. All rights reserved.

Résumé

Dans cette contribution, nous présentons un survol des résultats de recherche concernant la sensitivité des systèmes multiplexés à division de fréquence (OFDM) aux erreurs de synchronisation. Nous montrons que les systèmes OFDM sont assez sensibles à l'offset de fréquence porteuse ainsi qu'à l'offset de fréquence d'horloge: Dans la présence de ces détériorations, le rapport signal à bruit (SNR) calculé à l'entrée de l'outil de décision est une fonction décroissante du nombre de porteuses. Comparés aux systèmes classiques à porteuse unique, les systèmes OFDM ont la même sensitivité au jitter de phase de porteuse et une sensitivité au jitter d'horloge quelque peu plus grande. © 2000 Elsevier Science B.V. All rights reserved.

Keywords: Telecommunication; OFDM; Carrier synchronization; Clock synchronization

* Corresponding author. Fax: + 32-9-264-4295.

E-mail address: marc.moeneclaey@telin.rug.ac.be (M. Moeneclaey).

0165-1684/00/$ - see front matter

PII: S0165-1684(00)00031-1

Nomenclature

OFDM	orthogonal frequency-division multiplexed
$p_{tr}(t)$	transmit pulse
α	rolloff factor
$P_{tr}(f)$	transmit filter transfer function
$P_{rec}(f)$	receive filter transfer function
$H_{ch}(f)$	channel transfer function
$s_{m,k}$	mth transmit sample during kth symbol interval
$a_{n,k}$	kth symbol on nth carrier
$1/T$	pulse transmission rate
N	number of carriers
νT	length of cyclic prefix
$\phi_{m,k}$	carrier phase error associated with mth sample during kth symbol interval
$S_\phi(f)$	carrier phase jitter spectrum
σ_ϕ^2	carrier phase jitter variance
ΔF	carrier frequency offset
$\varepsilon_{n,k}$	normalized timing error associated with mth sample during kth symbol interval
$S_\varepsilon(f)$	timing jitter spectrum
σ_ε^2	timing jitter variance
$\Delta T/T$	normalized clock frequency offset
$I_{n,i,k}$	interference from ith carrier on nth FFT output during kth symbol interval
SNR_n	SNR at nth FFT output
D_n	degradation of SNR at nth FFT output

1. Introduction

In an orthogonal frequency-division multiplexed (OFDM) system, a parallel transmission of N data symbols per symbol interval is realized, by modulating the data on N orthogonal carriers [1,9].

Orthogonal frequency-division multiplexed (OFDM) systems have been proposed, standardized and/or implemented for various applications, such as high-speed data transmission over twisted-pair cables [2] and broadcasting of digital audio and digital TV [1]. The popularity of OFDM systems comes from their high immunity to channel dispersion, as compared to traditional single-carrier (SC) systems. The SC systems are usually equalized by means of time-domain equalizers; such equalizers become highly complex (many interacting taps, yielding slow convergence) when the channel impulse response is much longer than the symbol duration. On the other hand, for the OFDM systems each individual carrier is equalized by means of a single tap, which compensates for the attenuation and phase shift experienced by the considered carrier [1,9]. However, as compared to SC systems, OFDM systems are more sensitive to amplifier nonlinearities [3].

In this contribution, we investigate the sensitivity to synchronization errors of OFDM systems. The description of the OFDM system is presented in Section 2. In Section 3, we consider the effect of a carrier phase offset and a timing offset. In Sections 4 and 5 we compute the degradation of the signal-to-noise ratio at the input of the decision device, caused by carrier frequency offset, carrier phase jitter, clock frequency offset and timing jitter, and a comparison with single-carrier systems is carried out. Conclusions are drawn in Section 6.

2. System description

The complex envelope $s(t)$ of the transmitted OFDM signal is given by

$$s(t) = \sum_{k=-\infty}^{+\infty} \sum_{m=-\nu}^{N-1} s_{m,k} p_{tr}(t - k(N+\nu)T - mT), \quad (1)$$

where $p_{tr}(t)$ denotes the transmit pulse and $1/T$ is the pulse transmission rate. For $m \in (-\nu, N-1)$, the quantities $\{s_{m,k}\}$ are given by

$$s_{m,k} = \sum_{n=0}^{N-1} a_{n,k} \exp(\mathrm{j}2\pi(nm/N)) \quad (2)$$

and can be interpreted as a sequence of samples, taken at the rate $1/T$, of the continuous-time multicarrier signal $\sum_{n=0}^{N-1} a_{n,k} \exp(\mathrm{j}2\pi(nt/NT))$. In (2), $a_{n,k}$ is the kth symbol transmitted on the nth carrier; the frequency f_n of the nth carrier equals $n/(NT)$, and N denotes the number of carriers. It follows from (2) that the N samples $\{s_{m,k} | m = 0, \ldots, N-1\}$ are the IFFT of the N symbols $\{a_{nk} | n = 0, \ldots, N-1\}$, while $\{s_{m,k} | m = -\nu, \ldots, -1\} = \{s_{m,k} | m = N-\nu, \ldots, N-1\}$: the first ν samples constitute a cyclic prefix, i.e. a duplication of the last ν samples. The duration νT of the cyclic prefix is called the guard interval. The symbol rate per carrier, R_{ca}, is given by $R_{ca} = 1/(N+\nu)T$.

The OFDM transmitter block diagram is shown in Fig. 1. The N parallel data streams, each having rate R_{ca}, are applied to an IFFT processor, which computes the N-points IFFT of the N data symbols belonging to the same symbol interval. The IFFT output is serialized by means of a parallel-to-serial (P/S) conversion, which yields the transmit samples $\{s_{m,k}|m = 0,\dots,N-1\}$ at the rate NR_{ca}. To these samples the cyclic prefix $\{s_{m,k}|m = -\nu,\dots,-1\}$ is added, which gives rise to the transmit samples $\{s_{m,k}|m = -\nu,\dots,N-1\}$ at rate $1/T$. These samples are applied to the transmit filter with impulse response $p_{tr}(t)$ to produce the complex envelope $s(t)$ of the transmitted OFDM signal.

Let us assume that the samples $\{s_{m,k}\}$ are applied to a filter with transfer function $H(f)$, whose impulse response duration does not exceed the guard interval νT. Then it can be verified that the N samples $\{x_{m,k} = x(k(N+\nu)T + mT)|m = 0,\dots,N-1\}$ of the signal $x(t)$ at the output of the filter $H(f)$ are given by

$$x_{m,k} = \sum_{n=0}^{N-1} a_{nk} H_n \exp(\,j2\pi(nm/N)), \tag{3}$$

where

$$H_n = \frac{1}{T}\sum_{i=-\infty}^{+\infty} H\left(\frac{n}{NT} + \frac{i}{T}\right). \tag{4}$$

This means that the transient at the edges of the kth symbol interval does not affect the samples $x_{m,k}$ for $m = 0,\dots,N-1$, as illustrated in Fig. 2 which shows the envelope of the nth carrier during the kth symbol interval, observed at the input and the output of the filter $H(f)$. It follows from (3) that the N samples $\{x_{m,k}|m = 0,\dots,N-1\}$ are the IFFT of the sequence $\{a_{nk}H_n|n = 0,\dots,N-1\}$.

This motivates the receiver structure from Fig. 3, where the coefficients H_n are related to the end-to-end transfer function $H(f) = P_{tr}(f)H_{ch}(f)P_{rec}(f)$, with $P_{tr}(f)$, $H_{ch}(f)$ and $P_{rec}(f)$ denoting the tranfer functions of the transmit filter, the channel and the receive filter. The received complex envelope $r(t)$ is applied to the receive filter $P_{rec}(f)$, and sampled at the pulse transmission rate $1/T$. Each symbol interval consists of $N+\nu$ samples, but the prefix of ν samples, which might be affected by the transients due to the transfer function $H(f)$, is disregarded. The remaining N samples of the symbol interval, which are not affected by the transients, are converted from serial to parallel (S/P) and applied to an N-point FFT processor, which operates at a rate of one FFT per $1/R_{ca}$ seconds. The useful component at the nth FFT output during the kth symbol interval equals $a_{n,k}H_n$, which indicates that the constellation points are rotated over an angle $\arg(H_n)$ and scaled by a factor $|H_n|$. This linear distortion is compensated by means of a single tap

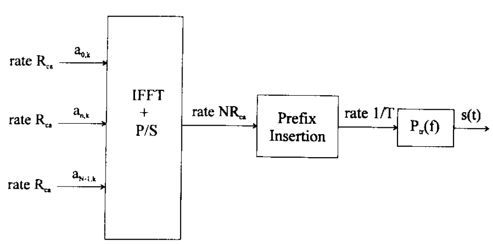

Fig. 1. OFDM transmitter block diagram.

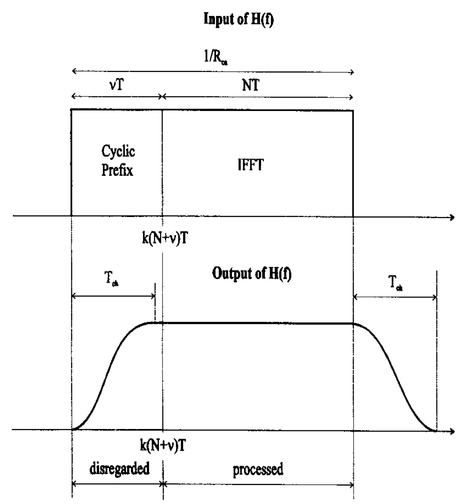

Fig. 2. Envelope of nth carrier during kth symbol interval.

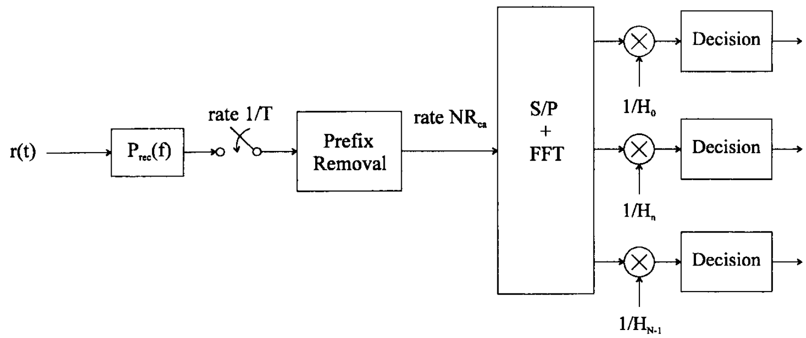

Fig. 3. OFDM receiver block diagram.

equalization per carrier: before making a symbol decision, the nth FFT output is multiplied by $1/H_n$ which corresponds to a rotation over an angle -arg(H_n) and a scaling by $1/|H_n|$. However, equalization considerably enhances the noise for strongly attenuated carriers.

3. Carrier phase offset and timing offset

The case of a constant carrier phase error ϕ at the input of the FFT can be investigated by incorporating the phase error into the end-to-end transfer function. Denoting by $H(f,\phi)$ the end-to-end transfer function that corresponds to a constant carrier phase error ϕ, we obtain

$$H(f,\phi) = H(f,0)\exp(j\phi) \tag{5}$$

from which it follows that

$$H_n(\phi) = H_n(0)\exp(j\phi), \tag{6}$$

where $H_n(\phi)$ denotes the coefficient that is related to $H(f,\phi)$ through (4). Hence, a constant carrier phase error ϕ yields a pure rotation of the useful signal component at each FFT output over an angle ϕ, as compared to the case $\phi = 0$. This is compensated by simply rotating the FFT outputs over (an estimate of) $-\phi$. As the noise power is not affected by this rotation, the signal-to-noise ratio (SNR) at the input of the decision device is not degraded by this compensation.

The case of a constant timing error εT at the input of the FFT can be investigated by incorporating the timing error into the end-to-end transfer function. Denoting by $H(f,\varepsilon)$ the end-to-end transfer function that corresponds to a constant timing error εT, we obtain

$$H(f,\varepsilon) = H(f,0)\exp(-j2\pi f\varepsilon T). \tag{7}$$

Now let us assume that $H(f,0) = 0$ for $|f| > (1+\alpha)/(2T)$, with $0 < \alpha < 1$. Denoting by $H_n(\varepsilon)$ the coefficient that is related to $H(f,\varepsilon)$ through (4), we obtain

$$H_n(\varepsilon) = H_n(0)\exp\left(-j2\pi\varepsilon\frac{\mathrm{mod}\,(n,N)}{N}\right),\quad \frac{n}{T}\notin\left(\frac{1-\alpha}{2T},\frac{1+\alpha}{2T}\right),$$
$$|H_n(\varepsilon)| < |H_n(0)|,\quad \frac{n}{T}\in\left(\frac{1-\alpha}{2T},\frac{1+\alpha}{2T}\right), \tag{8}$$

where mod(x, N) is the modulo-N reduction of x, yielding a result in the interval $(-N/2, N/2)$. The frequency interval $((1-\alpha)/(2T), (1+\alpha)/(2T))$ is the region of overlap between $H(f,0)$ and $H(f-1/T,0)$, and is denoted as the rolloff area. Hence, for carrier frequencies n/T *outside* the rolloff area the useful signal component at the corresponding FFT output is rotated over an angle $-2\pi\varepsilon\,\mathrm{mod}\,(n,N)/N$ as compared to the case $\varepsilon = 0$; this can be compensated without performance loss by rotating the nth

FFT output over (an estimate of) the angle $2\pi\varepsilon \bmod (n, N)/N$. Contrarily, for carrier frequencies n/T *inside* the rolloff area, the useful signal component at the corresponding FFT output is not only rotated over some angle, but also *attenuated* as compared to the case $\varepsilon = 0$; this means that a constant timing error yields an inevitable reduction of the SNR for carriers within the rolloff area. The dependence of $|H_n(\varepsilon)|$ on the carrier index n is illustrated in Fig. 4, assuming that $H(f, 0)$ has a cosine rolloff shape with $\alpha = 0.3$. Note that the reduction of the carriers within the rolloff area gets worse with increasing ε; for $\varepsilon = \frac{1}{2}$, the carrier at frequency $1(2T)$ has completely disappeared.

The sensitivity of OFDM to constant timing errors is eliminated by not using any carriers in the rolloff area, i.e. $a_{n,k} = 0$ for $n/T \in ((1-\alpha)/(2T), (1+\alpha)/(2T))$. In this case, a constant timing err or can be compensated without reduction of the SNR by applying the appropriate rotation to each FFT output.

4. Carrier frequency offset and phase jitter [5–8]

In this section we investigate the effect of a carrier frequency offset and phase jitter on an OFDM *reference* system with the following properties:

- The transmit and receive filters are ideal lowpass filters with bandwidth $1/(2T)$.
- The channel transfer function satisfies $H_{ch}(f) = 1$, so that no linear distortion is introduced.
- The channel adds complex-valued white noise, with independent real and imaginary parts each having a power spectral density of $N_0/2$.
- For all carriers the energy per symbol equals E_s.
- As the cascade of transmit filter, channel and receive filter does not introduce linear distortion, the system uses no cyclic prefix ($\nu = 0$).
- As the system bandwidth of $1/(2T)$ gives rise to zero rolloff area, all N carriers are modulated

The case of OFDM systems deviating from this reference system is discussed in Section 6.

Let us consider a carrier phase error $\phi(t)$ at the input of the FFT, which is slowly time varying as compared to the sampling interval T. The following two cases will be investigated:

- *Carrier frequency offset*: The carrier phase error $\phi(t)$ is given by $\phi(t) = 2\pi\Delta F t$, where ΔF denotes the carrier frequency offset. We assume that $\Delta F T \ll 1$.
- *Carrier phase jitter*: The carrier phase jitter $\phi(t)$ is the phase error resulting from a PLL. This phase error is modeled as a zero-mean stationary process with spectrum $S\phi(f)$. We assume that $S\phi(f) = 0$ for $|f| > B$, with $BT \ll 1$.

In the presence of a time-varying carrier phase error, the signal at the nth FFT output can be written as

$$a_{n,k} I_{n,n,k} + \sum_{i \neq n} a_{i,k} I_{n,i,k} + N_{n,k}, \tag{9}$$

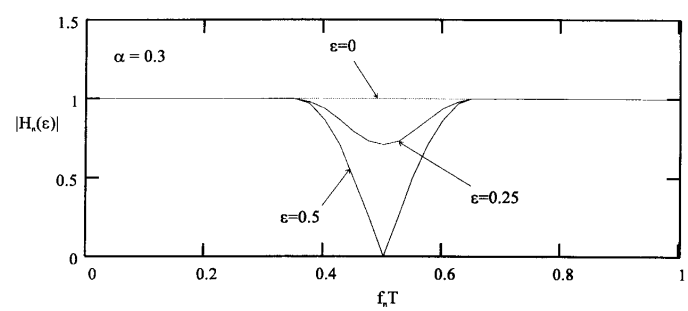

Fig. 4. Dependence of $|H_n(\varepsilon)|$ on the carrier index n.

where $N_{n,k}$ is a zero-mean complex-valued Gaussian noise term with $E[|N_{n,k}|^2] = N_0/E_s$,

$$I_{n,i,k} = \frac{1}{N}\sum_{m=0}^{N-1} \exp(\mathrm{j}\phi_{m,k})\exp(-\mathrm{j}2\pi(m(n-i)/N)) \tag{10}$$

and $\phi_{m,k} = \phi(mT + k(N+v)T)$. Note that $I_{n,i,k}$ is the FFT of $\{\exp(\mathrm{j}\phi_{m,k})\}$, evaluated at the frequency $(n-i)/N$. The quantity $I_{n,i,k}$ denotes the interference at the nth FFT output originating from the ith carrier during the kth symbol. When $\phi(t)$ is constant, we obtain $|I_{n,n,k}| = 1$ and $I_{n,i,k} = 0$, $i \neq n$, so that the signal-to-noise ratio (SNR) at each of the FFT outputs equals E_s/N_0. When $\phi(t)$ is not constant, we observe that

- $|I_{n,n,k}| < 1$, which indicates a reduction of the useful signal component
- $I_{n,i,k} \neq 0$ for $i \neq n$, which indicates the occurrence of intercarrier interference (ICI).

Hence, a time-varying carrier phase yields a reduction of the SNR at the FFT output.

When the carrier phase error is modeled as a random process, the quantity $I_{n,n,k}$ is a random variable, which we decompose as

$$I_{n,n,k} = E[I_{n,n,k}] + (I_{n,n,k} - E[I_{n,n,k}]). \tag{11}$$

The first term in (11) denotes the average useful component, whereas the second term is the random fluctuation of the useful component. Assuming that the receiver is able to accurately estimate $E[I_{n,n,k}]$, the nth FFT output is multiplied by $1/E[I_{n,n,k}]$, in order to compensate for the phase shift and scaling of the useful component.

In the presence of a time-varying carrier phase error, the SNR at the nth FFT output is given by

$$\mathrm{SNR}_n = \frac{E_s|E[I_{n,n,k}]|^2}{N_0 + E_s(E[|I_{n,n,k}|^2] - |E[I_{n,n,k}]|^2) + E_s E\left[\sum_{i\neq n}|I_{n,i,k}|^2\right]}. \tag{12}$$

It is clear from (12) that the reduction of the average useful component, the random fluctuation of the average component, and the occurrence of ICI degrade the SNR at the nth FFT output, as compared to the value E_s/N_0 that corresponds to the case of no carrier phase error. This degradation D_n, expressed in dB, is given by $10\log((E_s/N_0)/\mathrm{SNR}_n)$.

4.1. Carrier frequency offset

In the case of a carrier frequency offset ΔF, the quantities $I_{n,i,k}$ are deterministic, so there is no random fluctuation of the useful component. We obtain

$$|I_{n,i,k}| = \left|\frac{\sin(\pi(\Delta FT - (n-i)/N)N)}{N\sin(\pi(\Delta FT - (n-i)/N))}\right|. \tag{13}$$

From (10) it can be derived that

$$\sum_{n=0}^{N-1} |I_{n,i,k}|^2 = 1. \tag{14}$$

Using (14) and (13) in (12) yields the following expression for the degradation D_n:

$$\begin{aligned} D_n &= -10\log(|I_{n,n,k}|^2) + 10\log\left(1 + \frac{E_s}{N_0}(1 - |I_{n,n,k}|^2)\right) \\ &= -10\log\left(\left|\frac{\sin(\pi(\Delta FT)N)}{N\sin(\pi(\Delta FT))}\right|^2\right) \\ &\quad + 10\log\left(1 + \frac{E_s}{N_0}\left(1 - \left|\frac{\sin(\pi(\Delta FT)N)}{N\sin(\pi(\Delta FT))}\right|^2\right)\right). \end{aligned} \tag{15}$$

The degradation D_n does not depend on the carrier index, and is shown in Fig. 5. It follows that OFDM is very sensitive to a carrier frequency offset: in order to obtain a small degradation of the SNR, we need $\Delta F \ll 1/NT$ for OFDM, whereas we only need $\Delta F \ll 1/T$ for a traditional single-carrier system with symbol rate $1/T$. The degradation of the OFDM system, which originates because the FFT operates on a signal with carrier frequency offset, can be avoided only by applying carrier frequency correction *in front of* the FFT.

4.2. Carrier phase jitter

In the case of carrier phase jitter, the quantities $I_{n,i,k}$ are stationary processes. Assuming that

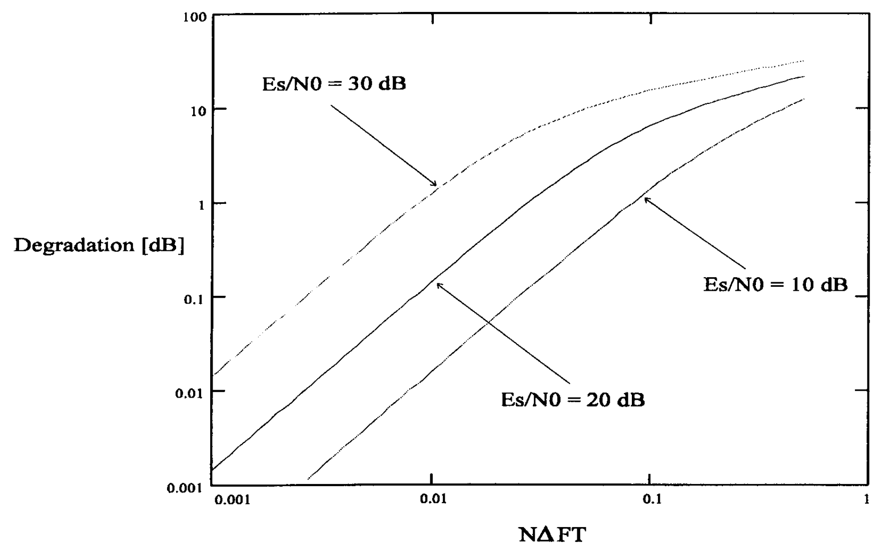

Fig. 5. Degradation caused by carrier frequency offset.

$\sigma_\phi^2 = E[\phi^2(t)] \ll 1$, we obtain

$$I_{n,n,k} \cong 1 + \mathrm{j}\frac{1}{N}\sum_{m=0}^{N-1} \phi_{m,k}, \tag{16}$$

$$I_{n,i,k} \cong \mathrm{j}\frac{1}{N}\sum_{m=0}^{N-1} \phi_{m,k} \exp(-\mathrm{j}2\pi(m(n-i)/N)), \quad i \neq n. \tag{17}$$

It follows from (16) that the useful component exhibits a random fluctuation, while (17) indicates the presence of ICI. Substituting (16) and (17) into (12), the resulting degradation of the SNR turns out to be the same for all carriers, and is given by

$$D_n = 10 \log\left(1 + \sigma_\phi^2 \frac{E_s}{N_0}\right) \quad \mathrm{dB} \tag{18}$$

which is independent of both the number N of carriers and the shape of the jitter spectrum $S_\phi(f)$. In obtaining (18), we have made use of $E[I_{n,n,k}] = 1$ and

$$\sigma_\phi^2 = E[|I_{n,n,k} - 1|^2] + E\left[\sum_{i \neq n} |I_{n,i,k}|^2\right] \tag{19}$$

which follow from (16) and (17).

Now, we consider a single-carrier system using square-root Nyquist transmit and receive filters. Assuming no channel distortion ($H_{\mathrm{ch}}(f) = 1$), the kth sample at the input of the decision device is given by

$$a_k \exp(\mathrm{j}\phi_k) + N_k \cong a_k(1 + \mathrm{j}\phi_k) + N_k, \tag{20}$$

where N_k is complex-valued additive noise with $E[|N_k|^2] = N_0/E_s$, and ϕ_k is the carrier phase jitter at the kth decision instant. Denoting the jitter variance by σ_ϕ^2, it follows from (20) that the degradations of the SNR for OFDM systems and for single-carrier systems are exactly the same. This degradation is shown in Fig. 6.

Although the degradations of the SNR for an SC system and an OFDM system are the same when both systems are subjected to the same carrier phase jitter variance, the effect of carrier phase jitter on the scatter diagram of SC and OFDM systems is very different.

In the case of SC, it follows from (20) that carrier phase jitter gives rise to a random rotation of the constellation, i.e. an angular displacement of the constellation points; the variance of this angular

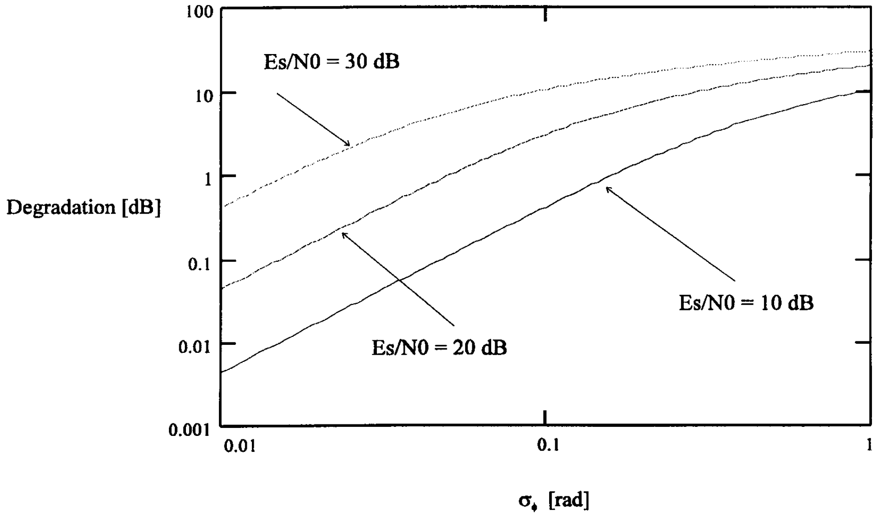

Fig. 6. Degradation caused by carrier phase jitter.

displacement equals the jitter variance. In the case of OFDM, the situation is more complicated. Taking (16) into account, it follows that the first term of (9) corresponds essentially to a random rotation of the signal constellation (angular displacement); the variance of this angular displacement is given by

$$E[|I_{n,n,k}-1|^2]=\int_{-\infty}^{+\infty}S_\phi(f)|H_N(\exp(\mathrm{j}2\pi fT)|^2\,\mathrm{d}f \tag{21}$$

with $H_N(\exp(\mathrm{j}2\pi fT))=\sin(\pi fNT)/N\sin(\pi fT)$ denoting the transfer function of a lowpass filter with bandwidth $1/(NT)$. The second term in (9) represents the ICI; in the scatter diagram, this term gives rise to circular clusters centered at the constellation points, i.e. the superposition of uncorrelated angular and radial displacements with equal variance $E[|\mathrm{ICI}|^2]/2$. Taking (19) and (21) into account, one obtains

$$E[|\mathrm{ICI}|^2]=\int_{-\infty}^{+\infty}S_\phi(f)(1-|H_N(\exp(\mathrm{j}2\pi fT)|^2)\,\mathrm{d}f. \tag{22}$$

It follows from (21) and (22) that $E[|I_{n,n,k}-1|^2]$ and $E[|\mathrm{ICI}|^2]$ both depend on the shape of the jitter spectrum; their sum equals the jitter variance, which is independent of the shape of the jitter spectrum. Hence, for a jitter spectrum with most of its power in the frequency range (0, $1/(NT)$), $E[|I_{n,n,k}-1|^2]$ is considerably larger than $E[|\mathrm{ICI}|^2]$, and the jitter essentially rotates the signal constellation. On the other hand, for a jitter spectrum with most of its power outside the frequency range (0, $1/(NT)$), $E[|I_{n,n,k}-1|^2]$ is considerably smaller than $E[|\mathrm{ICI}|^2]$, and the jitter essentially introduces ICI. This is confirmed by the following computer simulations. The considered jitter spectrum is shown in Fig. 7; the parameters f_L, f_H and $S_\phi(f_\mathrm{L})$ are related in such a way that $\sigma_\phi^2=(f_\mathrm{H}-f_\mathrm{L})S_\phi(f_\mathrm{L})$ for all simulations equals -21 dB rad^2. Fig. 8 shows the scatter diagram (without additive noise) for SC-QPSK; this diagram confirms the random rotation of the constellation, which is independent of the parameters f_L and f_H. Scatter diagrams (without noise) for OFDM-QPSK with 128 carriers are shown in Figs. 9 and 10, which correspond to $f_\mathrm{L}=0.01/T$, $f_\mathrm{H}=0.03/T$ and $f_\mathrm{L}=0.001/T$, $f_\mathrm{H}=0.03/T$, respectively. The difference between the two scatter diagrams for OFDM is explained by comparing the frequencies f_L and f_H with the

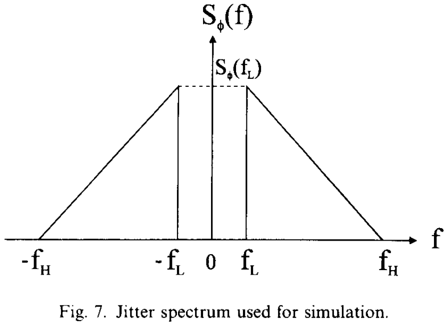

Fig. 7. Jitter spectrum used for simulation.

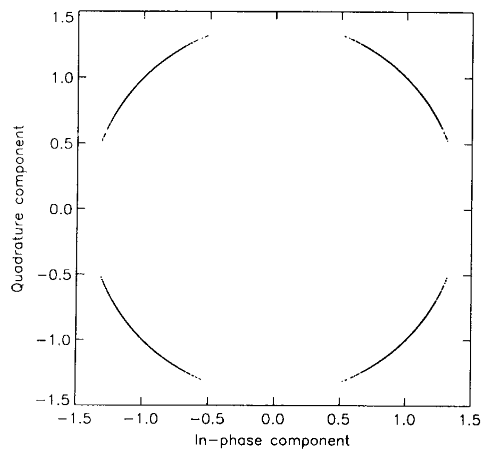

Fig. 8. Scatter diagram for SC-QPSK.

bandwidth $1/(NT) \cong 0.008/T$ of the lowpass filter $H_N(\exp(\mathrm{j}2\pi fT))$. All frequency components of the jitter used to produce Fig. 9 are above $1/(NT)$. Hence, ICI is the main disturbance, and the scatter diagram consists of circular clusters centered at the nominal constellation points. For the jitter giving rise to Fig. 10, about 40% and 60% of the jitter variance is caused by frequency components below and above $1/(NT)$, respectively. Hence, the variances of the radial and angular displacement in Fig. 10 are roughly $(60/2)\% = 30\%$ and $(60/2 + 40)\% = 70\%$ of the jitter variance, which explains the oval shape of the clusters.

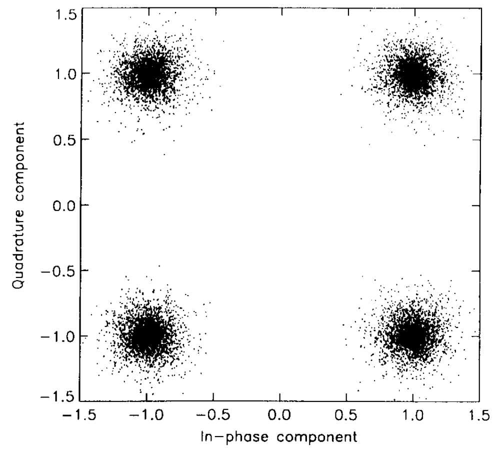

Fig. 9. Scatter diagram for OFDM-QPSK ($f_L = 0.01/T$, $f_H = 0.03/T$).

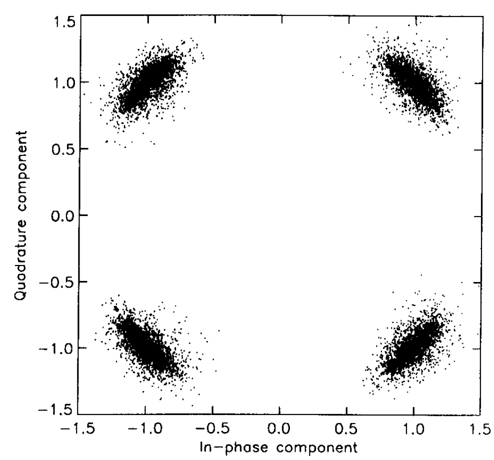

Fig. 10. Scatter diagram for OFDM-QPSK ($f_L = 0.001/T$, $f_H = 0.03/T$).

5. Clock frequency offset and timing jitter [4]

In this section we investigate the effect of a clock frequency offset and timing jitter on the OFDM reference system defined in Section 4. The case of OFDM systems deviating from this reference system is discussed in Section 6.

Let us assume that the mth sampling instant of the kth signal segment at the output of the receive filter deviates from the correct sampling instant $k(N+\nu)T+mT$ by an amount $\varepsilon_{m,k}T$, which is slowly varying as compared to the sampling interval T. The following two cases will be investigated:

- *Clock frequency offset*: Sampling is performed by means of a free-running clock with a relative frequency offset of $\Delta T/T$. Timing correction (rotation) is applied after the FFT. The normalized timing error $\varepsilon_{m,k}$ is given by $\varepsilon_{m,k}=m\Delta T/T$, where $\Delta T/T$ denotes the relative clock frequency offset. We assume that $\Delta T/T \ll 1$.
- *Timing jitter*: The normalized timing jitter $\varepsilon_{m,k}T$ is the normalized timing error resulting from a PLL. This timing error is modeled as a zero-mean stationary process with spectrum $S_\varepsilon(f)$. We assume that $S_\varepsilon(f)=0$ for $|f|>B$, with $BT \ll 1$.

In the presence of a slowly varying timing error, the signal at the nth FFT output can be written as (9), where now

$$I_{n,i,k}=\frac{1}{N}\sum_{m=0}^{N-1}\exp\left(j2\pi\varepsilon_{m,k}\frac{\text{mod}(i,N)}{N}\right)\times\exp\left(-j2\pi\frac{n-i}{N}\right). \quad (23)$$

Note that $I_{n,i,k}$ is the FFT of $\{\exp(j2\pi\varepsilon_{m,k}(\text{mod}(i,N)/N))\}$ taken at the frequency $(n-i)/N$. Comparing (10) with (23), it follows that a timing error $\varepsilon_{m,k}$ is equivalent to a carrier-dependent phase error $\phi_{n,m,k}$, given by $\phi_{n,m,k}=2\pi\varepsilon_{m,k}(\text{mod}(n,N)/N)$. When $\varepsilon_{m,k}$ is constant, we obtain $|I_{n,n,k}|=1$ and $I_{n,i,k}=0, i\neq n$. When $\varepsilon_{m,k}$ is not constant, we observe that

- $|I_{n,n,k}|<1$, which indicates a reduction of the useful signal component,
- $I_{n,i,k}\neq 0$ for $i\neq 0$, which indicates the occurrence of intercarrier interference (ICI).

The SNR at the nth FFT output is defined as in (12), and the corresponding degradation D_n as compared to the case without timing errors is given by $10\log((E_s/N_0)/\text{SNR}_n)$.

5.1. Clock frequency offset

In the case of a normalized clock frequency offset $\Delta T/T$, we obtain

$$|I_{n,i,k}|=\left|\frac{\sin(\pi(n-i-\text{mod}\,(i,N)\Delta T/T))}{N\sin(\pi/N(n-i-\text{mod}\,(i,N)\,\Delta T/T))}\right|.$$

The degradation of the SNR at the input of the decision device is shown in Fig. 11, as a function of the carrier index n. We observe that the maximum degradation occurs for $n=N/2$. Fig. 12 shows this maximum degradation as a function of $N\Delta T/T$. It follows that OFDM is very sensitive to a clock frequency offset: in order to obtain a small

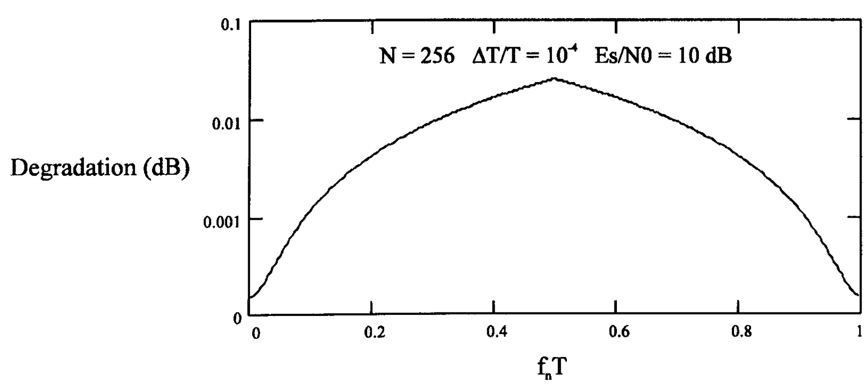

Fig. 11. Degradation caused by clock frequency offset: dependence on carrier index.

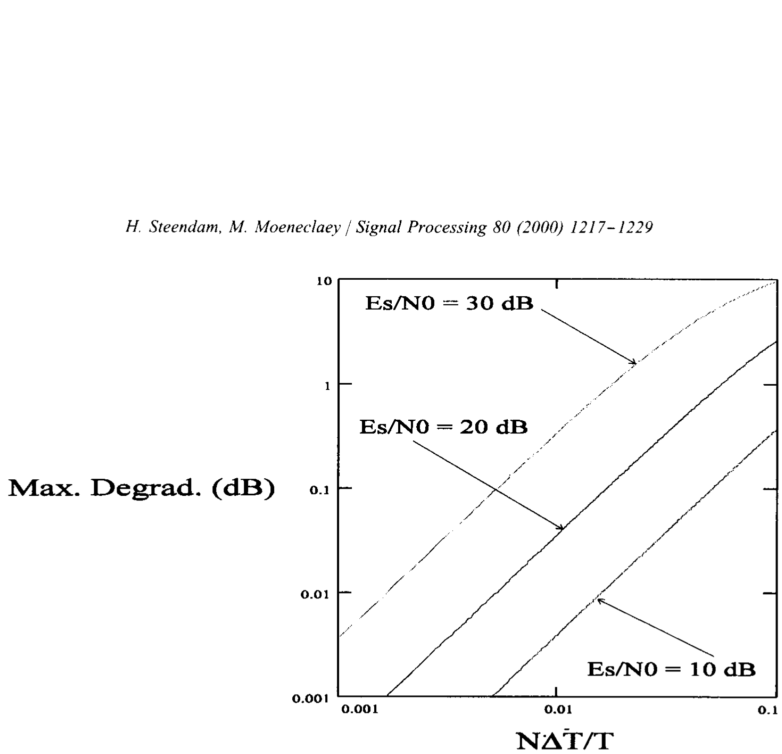

Fig. 12. Maximum degradation caused by clock frequency offset.

degradation of the SNR, we need $\Delta T/T \ll 1/N$ for OFDM, whereas we only need $\Delta T/T \ll 1$ for a traditional single-carrier system with symbol rate $1/T$. The degradation of the OFDM system, which originates because the FFT operates on a signal sampled with clock frequency offset, can be avoided only by applying timing correction *in front of* the FFT.

5.2. Timing jitter

In the case of timing jitter, the quantities $I_{n,i,k}$ are stationary processes. Assuming that $\sigma_\varepsilon^2 = E[\varepsilon_{m,k}^2] \ll 1$, we obtain

$$I_{n,n,k} \cong 1 + \mathrm{j}2\pi \frac{\mathrm{mod}\,(n,N)}{N}\left(\frac{1}{N}\sum_{m=0}^{N-1} \varepsilon_{m,k}\right), \tag{24}$$

$$I_{n,i,k} \cong \mathrm{j}2\pi \frac{\mathrm{mod}(i,N)}{N} \times\left(\frac{1}{N}\sum_{m=0}^{N-1} \varepsilon_{m,k} \exp\left(-\mathrm{j}2\pi m \frac{n-i}{N}\right)\right). \tag{25}$$

It follows from (24) that the useful component exhibits a random fluctuation about its mean value $E[I_{n,n,k}] = 1$, while (25) indicates the presence of ICI. The degradation of the SNR at the input of the decision device depends on the carrier index and on the shape of the jitter spectrum.

Let us consider the *average* SNR, which is obtained by replacing in (12) the quantities $|I_{n,i,k} - \delta_{n-i}|^2$ by their arithmetical average $(1/N)\sum_{n=0}^{N-1}|I_{n,i,k} - \delta_{n-i}|^2$ over all carriers; this corresponds to considering the average interference power over all carriers. The degradation D_{avg} of this average SNR turns out to be independent of the jitter spectrum and, for $N \gg 1$, independent of the number of carriers:

$$D_{\mathrm{avg}} = 10\log\left(1 + \frac{\pi^2}{3}\sigma_\varepsilon^2 \frac{E_\mathrm{s}}{N_0}\right) \quad N \gg 1. \tag{26}$$

Further, it can be verified that, in the case of uncorrelated timing jitter, the degradation D_n of SNR_n from (12) is the same for all carriers, and given by (26). In addition, also the maximum degradation $D_{\max}$ (maximum over all carrier indices and all jitter spectra) of SNR_n is independent of the number of carriers:

$$D_{\max} = 10\log\left(1 + \pi^2\sigma_\varepsilon^2 \frac{E_\mathrm{s}}{N_0}\right). \tag{27}$$

For a traditional single-carrier system that uses square-root Nyquist transmit and receive filters and operates on a non-distorting channel ($H_{\mathrm{ch}}(f) = 1$), the kth sample at the input of the decision device is given by

$$\sum_m a_{k-m} g(mT + \varepsilon_k T) + N_k \cong a_k + \varepsilon_k \sum_m a_{k-m} \dot{g}(mT)T + N_k, \qquad (28)$$

where $g(t)$ is a Nyquist pulse with $g(0) = 1$, $\dot{g}(t)$ is the derivative of $g(t)$, ε_k is the normalized timing error of the kth sampling instant, and N_k is zero-mean complex-valued noise with $E[|N_k|^2] = N_0/E_s$. The resulting degradation D_{sc} of the single-carrier system is given by

$$D_{avg} = 10 \log\left(1 + \left(\sum_m \dot{g}^2(mT)T^2\right)\sigma_\varepsilon^2 \frac{E_s}{N_0}\right). \qquad (29)$$

The degradations D_{avg} and D_{max} are shown in Fig. 13, along with the degradation D_{sc} of a single-carrier system with 30% rolloff. Note that the average degradation for OFDM is only slightly worse than the degradation of the single-carrier system.

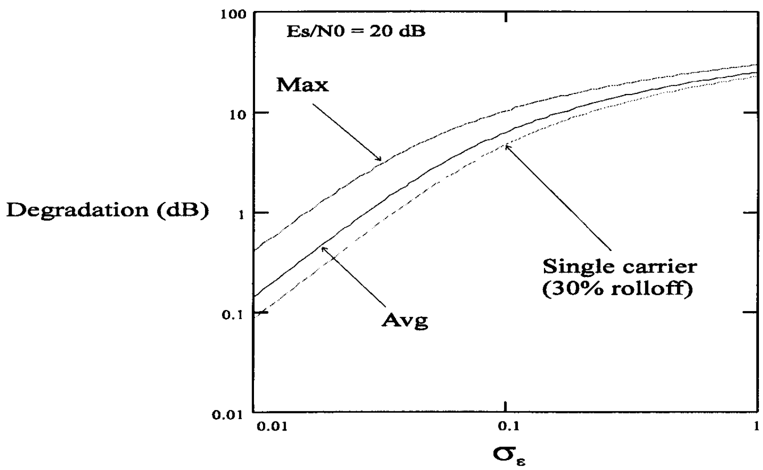

Fig. 13. Degradation caused by timing jitter.

Table 1
Effect of synchronization errors on OFDM reference system performance

Synchronization error	Degradation	Remarks
Constant phase error	No degradation	Yields pure rotation
Constant timing error	No degradation	Yields pure rotation
Carrier frequency offset	– same for all carriers – increases with N	Degradation avoided by correction in front of FFT
Phase jitter	– same for all carriers – independent of N	Degradation same as for single-carrier
Clock frequency offset	– depends on carrier index – increases with N	Degradation avoided by correction in front of FFT
Timing jitter	– depends on carrier index – independent of N	Average degradation similar to single carrier

6. Conclusions and remarks

In this contribution we have considered the effect of synchronization errors on the performance of an OFDM reference system. Carrier phase offset and timing offset at the input of the FFT can be compensated without performance loss by appropriate rotation of the FFT outputs. Performance is degraded when the carrier phase errors and timing errors at the input of the FFT are *time varying* over a symbol interval: these impairments yield a reduction of the useful component at the FFT output and give rise to ICI. Table 1 summarizes how the various synchronization errors affect the performance of the OFDM reference system.

The results presented in this paper pertain to the reference OFDM system. A practical OFDM system differs from the reference OFDM system: the transmit and receive filters have a non-zero rolloff, the channel gives rise to linear distortion. Therefore, a cyclic prefix is introduced, and the carriers in the rolloff area are not used. In the same way as for the reference OFDM system affected by synchronization errors, the SNR at the nth FFT output can be derived for the practical OFDM system. This SNR is given by

$$\mathrm{SNR}_n = \frac{E_{s,eq}(n)|E[I_{n,n,k}]|^2}{N_{0,eq}(n) + E_{s,eq}(n)(E[|I_{n,n,k}|^2] - |E[I_{n,n,k}]|^2) + \sum_{i\neq n} E_{s,eq}(i)E[|I_{n,i,k}|^2]}, \tag{30}$$

where the quantitiues $I_{n,i,k}$ are the same as for the OFDM reference system, while $E_{s,eq}(n)$ and $N_{0,eq}(n)$ denote the energy per symbol and the noise power spectral density for the nth carrier, both measured at the input of the FFT processor:

$$E_{s,eq}(n) = \frac{N}{N+\nu}E_s(n)\left|H_{ch}\left(\frac{\mathrm{mod}\,(n,N)}{NT}\right)\right|^2 \times \left|P_{rec}\left(\frac{\mathrm{mod}\,(n,N)}{NT}\right)\right|^2,$$

$$N_{0,eq}(n) = S\left(\frac{\mathrm{mod}\,(n,N)}{NT}\right)\left|P_{rec}\left(\frac{\mathrm{mod}\,(n,N)}{NT}\right)\right|^2. \tag{31}$$

In (31), $E_s(n)$ is the energy per symbol for the nth carrier, measured at the transmitter output, and $S(f)$ denotes the noise power spectral density at the input of the receiver. The factor $N/(N+\nu)$ accounts for the power loss due to disregarding the cyclic prefix at the receiver. By means of (30) and (31), the degradation of the SNR can be determined in terms of the various system and channel parameters. Qualitatively, the main conclusions resulting from the OFDM reference system remain valid for the practical OFDM system: as compared to single-carrier systems, OFDM systems are much more sensitive to carrier and clock frequency offset, and have a similar sensitivity to carrier phase and timing jitter.

References

[1] M. Alard, R. Lassalle, Principles of modulation and coding for digital broadcasting for mobile receivers, EBU Rev. 224 (August 1987) 3–25.
[2] J.S. Chow, J.-C. Tu, J.M. Cioffi, A discrete multitone transceiver for HDSL applications, IEEE J. Select. Areas Commun. SAC-9 (August 1991) 895–908.
[3] T. Pollet, M. Van Bladel, M. Moeneclaey, The effect of a nonlinear amplifier on the bit error rate performance of OFDM and single carrier signals, Proceedings of the EUSIPCO'94, Edinburgh, UK, September 1994, pp. 1548–1550.
[4] T. Pollet, P. Spruyt, M. Moeneclaey, The BER performance of OFDM systems using non-synchronized sampling, Proc. IEEE Global Telecommunications Conference, San Francisco, November 28–December 2, 1994, pp. 253–257.
[5] T. Pollet, M. Van Bladel, M. Moeneclaey, BER sensitivity of OFDM systems to carrier frequency offset and Wiener phase noise, IEEE Trans. Commun. COM-43 (February/March/April 1995) pp. 191–193.
[6] T. Pollet, M. Moeneclaey, I. Jeanclaude, H. Sari, The effect of carrier phase jitter on single-carrier and multi-carrier QAM systems, Proceedings of the IEEE International Conference on Communications ICC'95, Seattle, June 1995, pp. 1046–1050.
[7] T. Pollet, M. Moeneclaey, The effect of carrier frequency offset on the performance of bandlimited single carrier and OFDM signals, Proceedings of the IEEE Global Telecommunications Conference Globecom'96, London, 18–22 November 1996, pp. 719–723.
[8] H. Sari, G. Karam, I. Jeanclaude, Channel equalization and carrier synchronization in OFDM systems, Proceedings of the sixth Tirrenia International Workshop on Digital Communications, Tirrenia, Italy, September 1993, pp. 191–202.
[9] S.B. Weinstein, P.M. Ebert, Data transmission by frequency division multiplexing using the discrete Fourier transform, IEEE Trans. Commun. Technol. COM-19 (October 1971) 628–634.